March 2011

STRESS ORIENTATION DETERMINED FROM FAULT SLIP DATA IN HAMPEL WASH AREA, NEVADA, AND ITS RELATION TO CONTEMPORARY REGIONAL STRESS FIELD

Virgil A. Frizzell Jr.
U.S. Geological Survey

Mark D. Zoback
U.S. Geological Survey, zoback@stanford.edu

TECTONICS, VOL. 6, NO. 2, PAGES 89-98, APRIL 1987

STRESS ORIENTATION DETERMINED FROM FAULT SLIP DATA IN HAMPEL WASH AREA, NEVADA, AND ITS RELATION TO CONTEMPORARY REGIONAL STRESS FIELD

Virgil A. Frizzell, Jr.

U.S. Geological Survey, Flagstaff, Arizona

Mary Lou Zoback

U.S. Geological Survey, Menlo Park, California

Abstract. Fault-slip data were collected from an area of relatively young faulting in a seismically active part of the Nevada Test Site 12 km NW of Mercury, Nevada. The data come primarily from intensely faulted Miocene tuffaceous sedimentary rocks in Hampel Wash, which is bounded on the north by the Quaternary ENE trending Rock Valley fault and on the south by a parallel unnamed fault. Data from faults with known sense of displacement exhibit a bimodal distribution of slip angles (rakes). Faults exhibiting steep rakes (typically 75° to 90°) cluster about a N30°–35°E strike; most dip 65° to 80°. Faults having shallow rakes (generally less than 20°) exhibit a wide range of strikes (from N6°W to N80°E) and mostly dip between 80° and 90°. The predominant N30°–35°E strike of the steep-rake faults and the quasi-conjugate nature of a consistent subset of the shallow-rake faults suggest a maximum horizontal stress orientation of about N30°–35°E and a least horizontal principal stress direction of N55°–60°W. Analysis of the data using a least squares iterative inversion to determine a mean deviatoric principal stress tensor indicates a normal-faulting stress regime (S_1 vertical) with principal stress axes in approximately horizontal and vertical directions (S_1, trend = N19°E and plunge = 82°N; S_2, N30°E and 8°S; and S_3, N60°W and 2°E). The maximum horizontal stress, S_2, was found to be nearly intermediate in magnitude between S_1 and S_3. The N60°W least horizontal principal stress orientation obtained from the fault-slip inversion agrees with our geometric analysis of the data and is consistent with a modern least horizontal principal stress orientation of N50°–70°W inferred from earthquake focal mechanisms, well bore breakouts, and hydraulic fracturing measurements in the vicinity of the Nevada Test Site. This solution fits all the data well, except for a subset of strike-slip faults that strike N30°–45°E, subparallel to the normal faults of the data set. Nearly pure dip-slip and pure strike-slip movement on similarly oriented faults, however, cannot be accommodated in a single stress regime. Superposed sets of striae observed on some faults suggest temporal rotations of the regional stress field or local rotations within the region of the fault zone.

Paper number 6T0752.

INTRODUCTION

Much of the actively extending northern Basin and Range province appears characterized by a WNW least horizontal principal stress direction [Zoback and Zoback, 1980]. Wright [1976] subdivided the Basin and Range into two deforma tional fields having similar least horizontal principal stress directions: a northern field dominated by steeply dipping normal faults and a southern field featuring normal and strike-slip faults that formed coevally. Although Anderson and Ekren [1977] disputed Wright's sampling of late Cenozoic trends on the basis of more detailed fault relationships at several localities, they suggested a temporal clockwise change in the least horizontal stress orientation. Focal mechanism data [e.g. Vetter and Ryall, 1983] support Wright's relatively uniform orientation of the least horizontal principal stress direction as well as his suggestion that S_1 and S_2 (maximum and intermediate principal stress axes) may locally interchange.

In the vicinity of the Nevada Test Site, which is located in Wright's southern deformational field, a variety of structural and geomorphic data led Carr [1974, p. 10] to infer a N50°W least horizontal principal stress direction for deformation that began as early as 10 Ma and possibly as recently as 4 Ma. In a more recent structural analysis, Ander [1984] concurred with the present N50°W orientation. A paucity of dip-slip displacements on NE trending faults in the vicinity

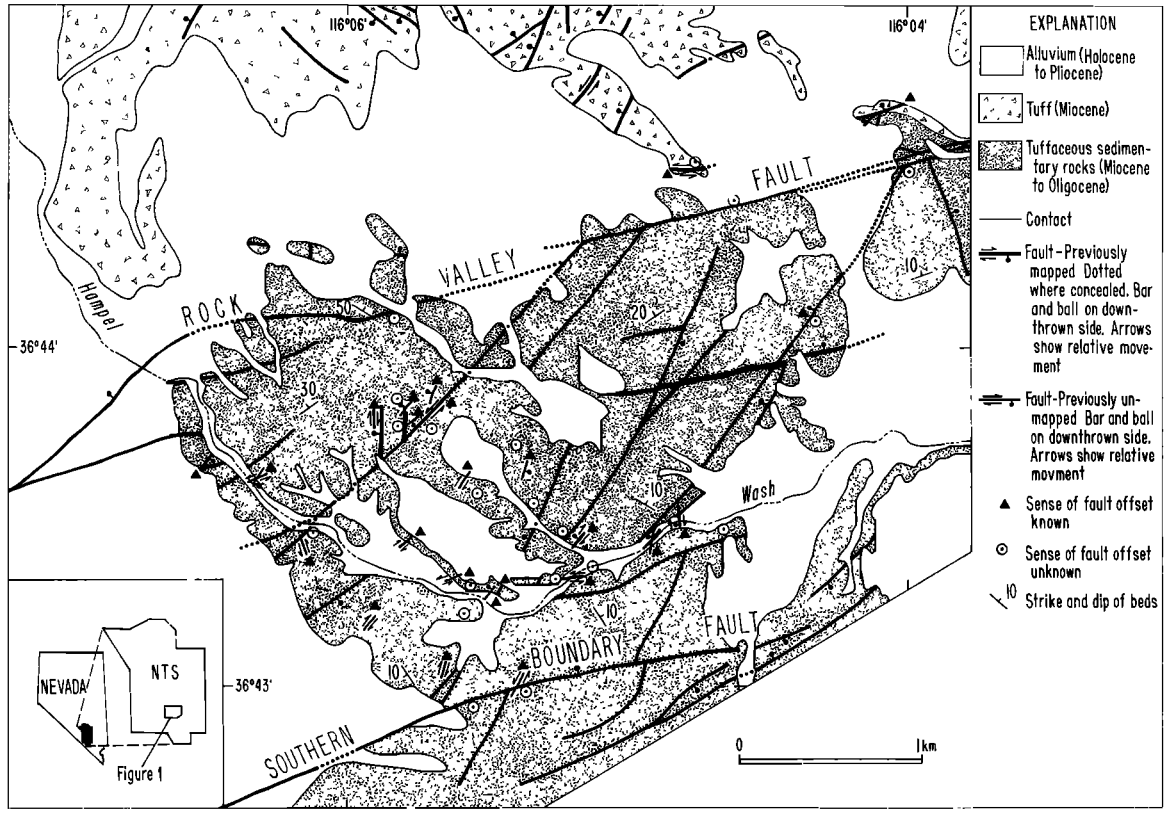

Fig. 1. Generalized geologic map of Hampel Wash area, Nevada Test Site, Nevada (after Hinrichs, 1968), showing locations from which fault slip data were obtained. Most data were collected from previously unmapped small faults that are depicted schematically. (a) All data collected along or near Rock Valley fault, (b) all data collected along southern bounding fault, (c) lower hemispheric equal area projection for all Hampel Wash data (n=160), (d) data collected from faults having known sense of displacement (n=50).

of Yucca Flat led Ander (p. 54) also to infer a "very recent" clockwise change in orientation of the least horizontal principal stress orientation from N78°W to the modern orientation of about N50°W.

Several other studies generally support Carr's inferred N50°W least horizontal principal stress orientation. These studies include earthquake focal mechanisms from the vicinity of the Nevada Test Site [Rogers et al., 1983], well bore breakouts from Pahute Mesa and Yucca Flat [Springer et al., 1984] and well bore breakouts and in situ stress (hydraulic fracturing) measurements [Stock et al., 1985] in the Yucca Mountain area, all of which indicate either normal or strike-slip faulting that has consistent least horizontal principal stress orientations of N50°–70°W.

East-northeast striking fault zones in a seismically active part of the Nevada Test Site [Rogers et al., 1983, Figure 1] have been designated as left-lateral strike-slip faults [Carr, 1974, Figure 3; 1984, p. 61]. Most faults having similar trends generally run along the axes of basins and are thus poorly exposed; therefore a thorough examination of their bedrock exposures and actual sense of movement has not been undertaken. The ENE trending Rock Valley fault and a parallel unnamed fault 2 km to the south indicate probable left-lateral oblique displacement of bedrock and cut Quaternary materials [Hinrichs, 1968; Barnes et al., 1982; Ander et al., 1984, pp. 16–17; Carr, 1984, p. 61; Yount et al., 1987]. These faults cut tuffaceous sedimentary rocks in the Hampel Wash area where outcrops eroded by ephemeral streams offer unique opportunities to examine exposures of the ENE trending presumed left-lateral fault zones as well as faults in the block bounded by them. This report presents the results of an analysis of fault slip data collected in the Hampel Wash area and modifies preliminary results summarized elsewhere [Frizzell and Zoback, 1985].

LOCAL GEOLOGIC SETTING

Significant stratigraphic and structural changes occur across the Hampel Wash area (Figure 1). These changes are even apparent on the state geologic map [Stewart and Carlson, 1978]. The wash itself is underlain by one of the older Tertiary units, the rocks of Pavits Springs of Hinrichs

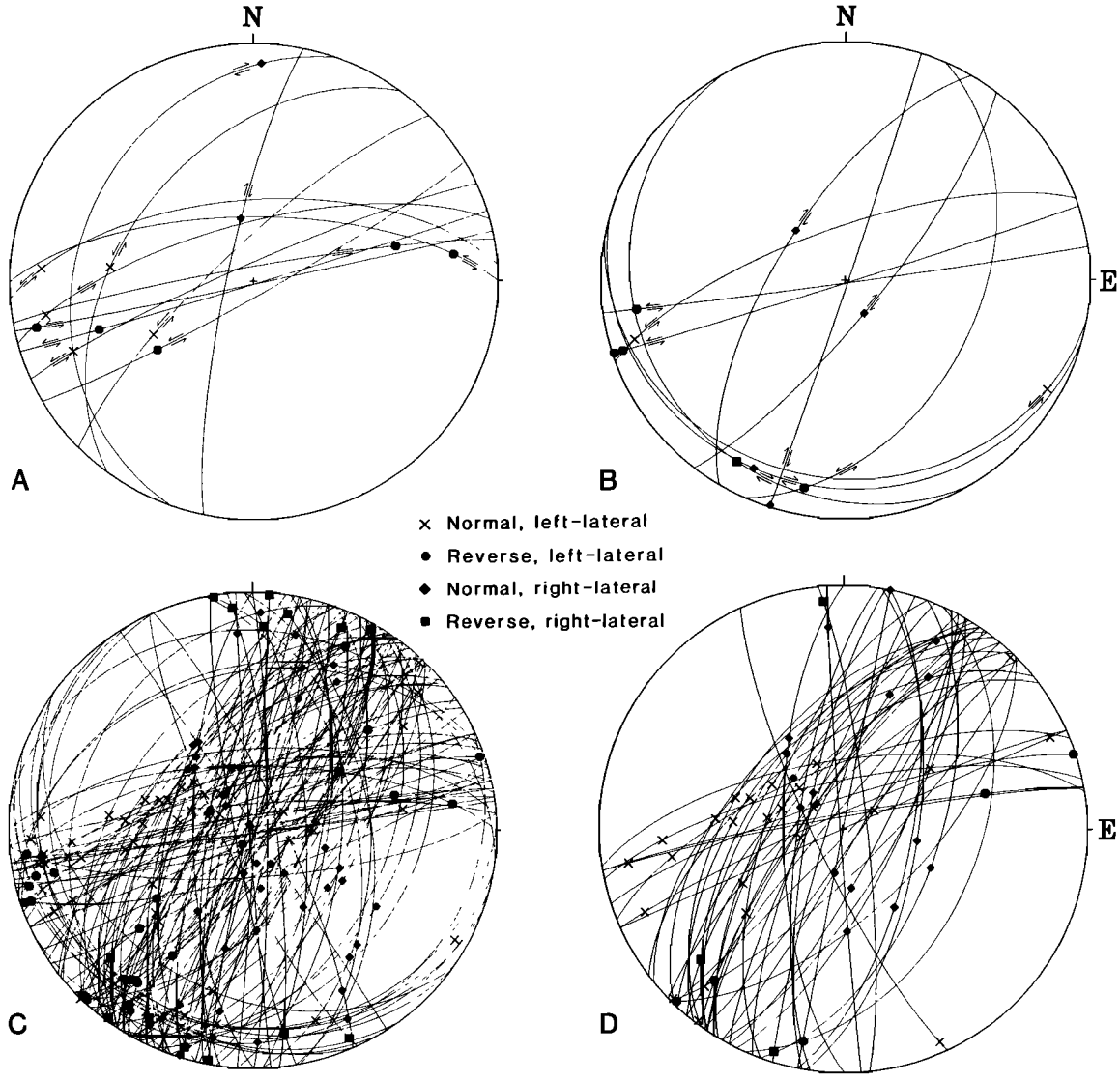

Fig. 1. (continued)

[1968]; these Miocene strata were deposited on the slightly older Horse Spring Formation. Paleozoic carbonate and clastic rocks [Burchfiel, 1964] unconformably underlie the Horse Spring Formation and occupy the ranges to the south and east; silicic ash fall tuffs and flows of Miocene and Pliocene age predominate in the ranges to the north [Byers et al., 1976]. Faults in the Paleozoic rocks south of the Hampel Wash area strike N60°–80°E, subparallel to the Rock Valley fault, but north of the wash, faults in the upper Tertiary rocks exhibit NNE to N trends.

The faults bounding the block that contains Hampel Wash displace numerous Neogene units. Although the amount of offset eludes exact measurement, lateral displacement probably is not greater than a few kilometers [Barnes et al., 1982]. The youngest volcanic unit that is directly offset, the Wahmonie Formation, yields potassium-argon ages of 12 and 13 Ma [Kistler, 1968]. Clasts of the younger [8 and 10 Ma, R. J. Fleck, written communication, 1980] basalt of Skull Mountain reside on the surfaces of beheaded alluvial fans of probable Pliocene age south of the physiographic Rock Valley [south of Figure 1; Hinrichs, 1968; J. C. Yount, oral commun., 1985]. These clasts, derived from the Skull Mountain area (north of Figure 1), must have traveled south across the present position of Rock Valley before the valley was formed. Thus, although the Rock Valley fault may be older than the fans, its topographic expression, and perhaps that of the southern boundary fault, apparently developed after about 5 Ma. Multiple events have occurred on the Rock Val-

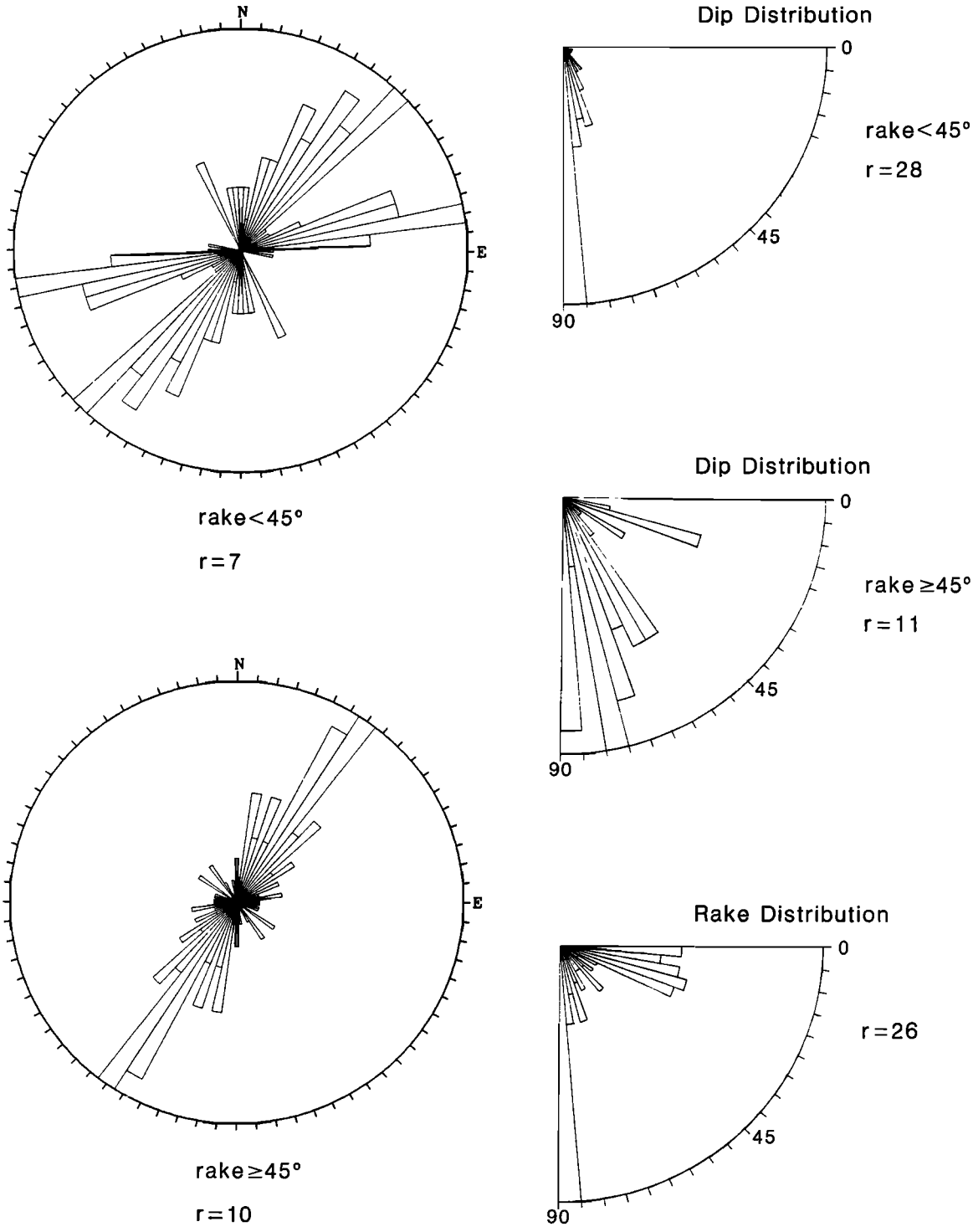

Fig. 2. Distributions of strike, dip, and rake for entire data set (n=160) of striae on faults in Hampel Wash area, Nevada, represented on Figure 1c.

ley fault over the past several hundred thousand years, and upper Pleistocene materials have been clearly offset [Yount et al., in press]. Although the fault creates prominent brushlines in Holocene deposits, actual breakage of Holocene materials has not been documented.

GEOMETRIC ANALYSIS OF FAULT PATTERNS

Exposures in Miocene tuff and tuffaceous sedimentary rocks yielded 160 orientations of striae on faults having measured displacements ranging from 4 cm to 1.7 m. Probable sense of displacement was determined for 50 of these features by using stratigraphic offset and macrostructures and microstructures discussed by Angelier et al. [1985, p. 351–353].

Most of the data were collected from small faults between the two ENE trending faults bounding the Hampel Wash area. Although fault slip data from the vicinity of the bounding faults represent a broad distribution of attitudes (see Figures 1a and 1b), most faults have shallowly plunging rakes. True sense of offset was not determined on any of the ENE trending faults along the bounding faults, however, apparent offset of rock units suggests that these bounding faults have a left-lateral oblique offset. If the displacement is consistently left lateral, then the slip data suggest both minor normal and reverse components of displacement on these near-vertical ENE trending faults.

The entire population of measurements from the Hampel Wash area is represented on a lower hemisphere equal-area projection in Figure 1c. Despite a broad distribution of fault attitudes, strike directions in the northeast quadrant dominate. Distributions of strike, dip, and slip angles (rakes) are shown in Figure 2 in two subsets of the data distinguished by rakes. Note that strike-slip faults (used herein for faults having rakes less than 45°) exhibit an apparent bimodal distribution of strike (N35°–45°E and N70°–80°E), whereas normal faults (faults with rakes greater than or equal to 45°) exhibit a unimodal distribution (N30°–35°E).

About a third of the measured faults, 50 of 160, exhibit characteristics that indicate true sense of displacement. Faults of this subset (Figure 1d) exhibit attitudes similar to those of the entire data set. Distribution of dip and rake (Figure 3) appears similar to that for the entire data set, with the exception that the shallowly dipping dip-slip faults are not included in this subset because their sense of displacement was not determined in the field.

Shallow-rake (strike-slip) faults having a known sense of offset exhibit a wide range in strike (Figure 3), although they can be divided into two nearly distinct fields (Figures 3 and 4). Faults having right-lateral offsets strike N to NE (N6°W to N36°E), whereas left-lateral faults strike NE to ENE (N36°E–80°E). Two left-lateral faults, numbered on Figure 4 with their slip directions circled, are exceptions to this general pattern and may represent measurement errors. Roughly half (11 of 25) of the measured strike-slip faults strike N28°–45°E, subparallel with the predominant strike direction of the dip-slip faults in the data set. These faults are discussed in detail in the section on discordant data.

A simple geometric analysis of the data permits a qualitative estimate of the principal stress orientations. The predominant N30°–35°E strike of the dip-slip faults and the quasi-conjugate nature of the northerly (right-lateral) and ENE striking (left-lateral) faults suggest a maximum horizontal principal stress orientation of N30°–35°E and a least horizontal principal stress orientation of N55°–60°W. Clearly, the NE striking strike-slip faults (both right- and left-lateral) are inconsistent with this simple stress regime.

QUANTITATIVE ESTIMATION OF PRINCIPAL STRESS ORIENTATION

Because the 50 faults having a known sense of offset are representative of the complete data set (compare Figures 1c, 1d, 2, and 3) and constitute the best data collected, they were analyzed by using a least squares iterative inversion outlined by Angelier [1984] to determine the mean deviatoric principal stress tensor. This method of analysis determines the parameters which define the direction of slip on a fault plane, i.e., the orientation of the principal stress axes and a ratio of relative stress magnitudes $\phi = (S_2 - S_3)/(S_1 - S_3)$, by minimizing the mean angular deviation between the computed and observed slip vector on each fault.

Because the iterative inversion process requires a "starting point" stress regime to compute slip directions for comparison with the observed fault slip data, the data were subjected to two inversions: one with an initial "normal dip-slip faulting" stress regime (S_1 vertical) and one with an initial "strike-slip faulting" stress regime (S_2 vertical). Both regimes were assigned a consistent least horizontal principal stress (S_3) orientation of N60°W. Starting with a normal-faulting stress regime, inversion of the data set having a known sense of motion converged rapidly on the "final" solution (S_1, N19°E trend and 82°N plunge; S_2, N30°E and 8°S; S_3, N60°W and 2°E) and a $\phi = 0.47$. Starting with a strike-slip faulting stress regime (S_2 vertical), the inversion yielded a N58°W orientation for the S_3 axis, essentially identical to that derived from the normal-faulting inversion. However, the best fitting ϕ value was 1.0, implying that the maximum horizontal principal stress magnitude equals the vertical stress ($S_1 = S_2$), or a stress regime transitional between strike-slip and normal faulting. Hence, the iterative solution for an initial strike-slip stress regime moved as close as allowed to a "normal-faulting" solution. Significantly, the "best" strike-slip faulting solution had a higher deviation angle between observed and computed rakes (34°) than did the normal-faulting solution (31°), indicating that the best fit to the overall data set was the normal-faulting regime with $\phi = 0.5$.

Additional inversion of the data set weighted by increasing amount of displacement [Angelier et al., 1985, p. 351] yielded similar ϕ values and principal stress axes that differed by less than 1°. Thus the S_3 axis determined from the fault data approximates a least horizontal principal stress direction of about N60°W, which compares favorably with other estimates of the contemporary stress field based on focal mechanisms, well bore breakouts, and hydraulic fracturing.

The goodness of fit of the normal-faulting solution with a $\phi = 0.5$ can be evaluated from the distribution of deviation angles between the observed and computed rakes (Figure 5). As noted above, the mean deviation angle for this solution was 31°; by ignoring the two inconsistent NNW trending left-lateral strike-slip faults discussed earlier which may represent measurement errors, this mean angle reduces to 27°.

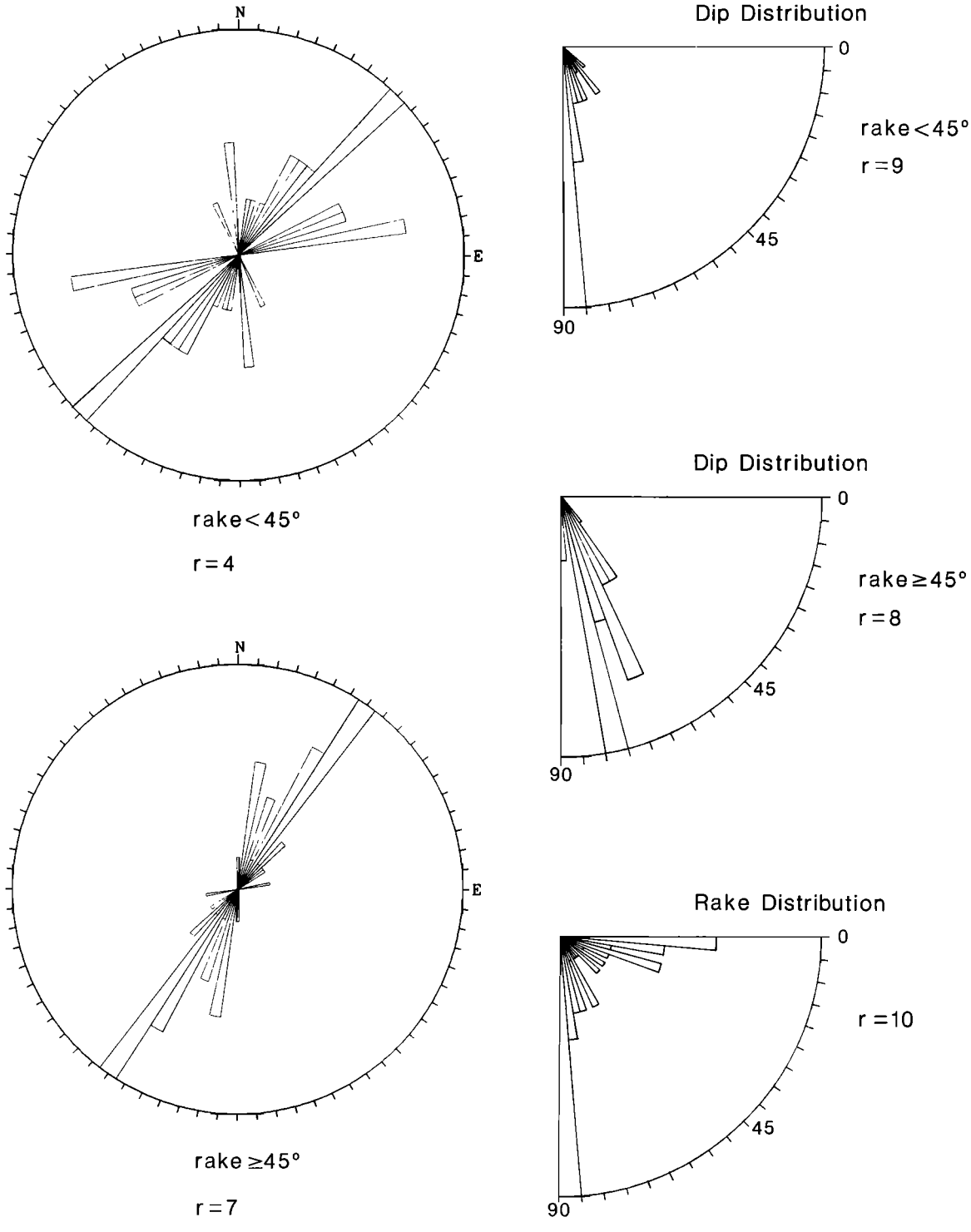

Fig. 3. Distributions of strike, dip, and rake for subset (n=50) of faults having known sense of displacement in Hampel Wash area, Nevada, represented on Figure 1d.

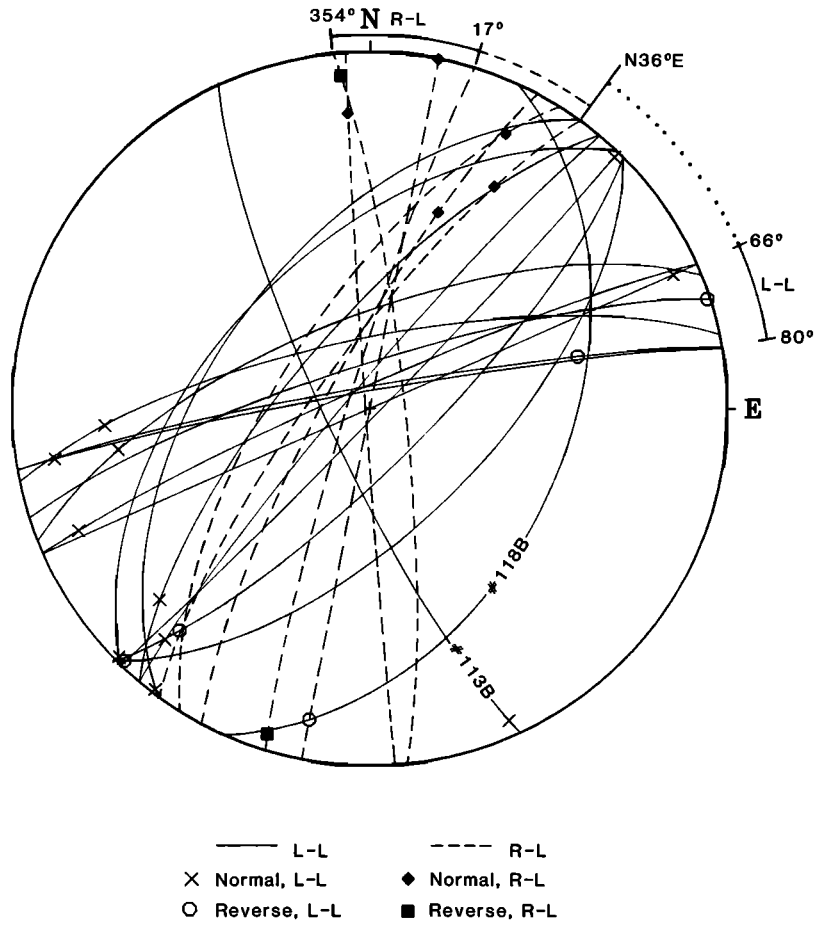

Fig. 4. Lower hemispheric equal-area projection of fault straie data from strike-slip (R-L right-lateral, L-L left-lateral) faults in Hampel Wash area, Nevada. See Figure 3 for rose diagrams of the same data.

Eighteen percent of the measured striae (nine of 50) exhibit orientations discordant (deviate by more than 45°) with the best solution. Exclusion of the discordant data (discussed below) yields a smaller mean deviation angle of 22°, indicating that the solution represents a good fit to most of the data.

DISCORDANT FAULT DATA

As anticipated, the shallow-rake faults that strike between N32°–45°E exhibit slip directions completely discordant (predicted slip directions that differ by 70° or more from observed direction) with the solution obtained by the inversion. This result was predictable because these strike-slip faults parallel the dip-slip faults of the data set.

Superposed sets of strike-slip and dip-slip striations were observed on four steeply dipping fault surfaces in this strike range (Table 1), but the relative age of the striations was not determined. Steep dips characterize the four faults, and

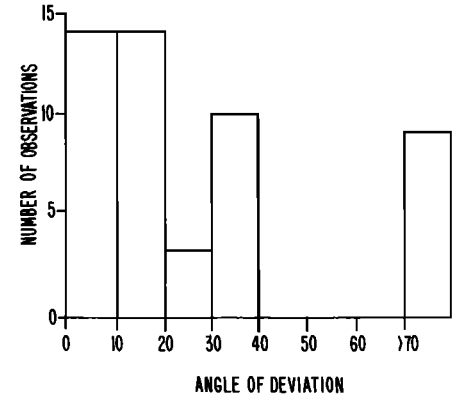

Fig. 5. Distribution of deviation angles between rakes observed in the field and theoretical rakes determined from the computer-derived solution.

TABLE 1. Superposed Sets of Striae on Fault Surfaces in Hampel Wash Area, Nevada

Fault	Strike, N°E	Dip, deg.	Rake, deg.	Deviation angle, deg.*
107B	14	90	17S	--
107B′	14	90	48S	--
174B	36	78W	90	11
174B′	36	78W	30N	71
174D	32	69W	85S	7
174D′	32	69W	16N	72
176A	23	90	22S	--
176A′	23	90	90	--

Sense of offset determined only for faults 174B and 174D (see text and Figure 6).

*Angle between measured rakes and those theoretically determined from solution.

very steep rakes (about 85°) represent the dip-slip motion on three of the four. The slip sense was determined on two fault surfaces (Table 1 and Figure 6, 174B and 174D) located along the same N30°–35°E-striking fault zone in Hampel Wash. Both exhibit normal right-lateral oblique senses of displacement. Although the steep orientations of striae may, in other circumstances, represent local "block settling" rather than a direct response to regional tectonic stress, this does not appear to be the case here because, given N30°–35°E the fault orientation, these steep rakes fit the solution discussed above.

A second subset of the data (10 of 50) yielded angles of 30° to 40° between the observed and predicted slip directions. These faults include N to NNE and ENE striking faults having steep rakes (greater than 80°) plus additional shallow-rake faults striking N17°–44°E. The solution that best fits the bulk of the data (S_3, N60°W; S_1, approximately vertical; and $\phi = 0.5$) predicts that faults having strikes of N20°–45°E would be expected to show primarily dip-slip displacements, whereas steep faults striking approximately N-S should be right lateral, and ENE faults should be primarily left lateral. Both the measured dip-slip displacements on NNE and ENE faults and, in particular, the strike-slip displacements on faults striking N20°–45°E very likely would not have occurred under the inferred stress regime and suggest either temporal variation in the regional stress field or local block rotations. Such variations are also indicated by the superposed dip-slip and strike-slip striae described above.

DISCUSSION

The orientation of the stress axes computed from fault slip data collected in the Hampel Wash area agrees with the current regional state of stress inferred from earthquake focal mechanisms, well bore breakouts, and hydraulic fracturing measurements for the Nevada Test Site area (summarized by Stock et al., [1985, table 3]). Because these indicators variously reflect normal and strike-slip faulting regimes having nearly uniform least horizontal principal stress direction of extension, they lend credence to Wright's [1976] model in which the least horizontal stress orientation remains constant and the maximum horizontal and vertical stress exchange magnitudes to explain the coeval existence of normal and strike-slip faulting in the region of the southern Basin and Range.

Such mixed-mode patterns of faulting have been reported by Angelier et al. [1985] at Hoover Dam, Nevada, 140 km SE of Hampel Wash. Fault data at Hoover Dam have been interpreted to indicate two late Cenozoic (about 12 to 5 Ma) deformational events, with a 55° clockwise rotation of S_3 between the two deformational events. Both of their deformational events involved a combination of normal dip-slip and strike-slip faulting as indicated by a bimodal distribution of rakes. Angelier et al. interpreted these data as indicating that the maximum horizontal and the vertical stress alternate without affecting the orientation of S_3 [Angelier et al., 1985, p. 361]. Our data set also exhibits a nearly bimodal distribution of rakes. However, the solution obtained on our data set indicates that both the normal dip-slip faulting and slip

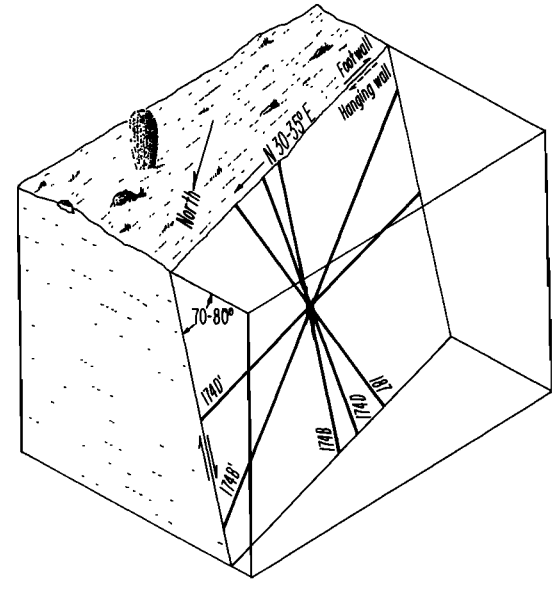

Fig. 6. Representation of two fault surfaces exhibiting superposed sets of striae (see Table 1). Striae 174B and 174D fit the solution (least horizontal principal stress orientation of N60°W), and striae 174B' and 174D' are discordant. For comparison, striation 187 (N34°E strike, 76°W dip, 48°S rake) represents a striation on a third fault surface that deviates 38° from the orientation theoretically predicted from the solution.

on the strike-slip faults of the "quasi-conjugate" N-to-NNE and ENE-to-E sets generally agree with the normal-fault solution with a $\phi = 0.47$. The deviation angles between actual and predicted slip for these quasi-conjugate strike-slip faults varied between 0° and 40° and had a mean value of 17°, a value somewhat lower than the overall misfit of the entire data set. The deviation angle for the dip-slip subset of the entire data set ranged from 1° to 40° with a mean value of 16°.

Thus the mixed strike-slip and dip-slip faulting in Hampel Wash may be explained simply in terms of a single deformational event in a normal faulting stress regime with a $\phi = \approx 0.5$ (the maximum horizontal stress intermediate in magnitude between S_3 and the vertical stress). Our limited data set does not require temporal variations of the relative magnitude of the maximum horizontal and vertical stress suggested by Wright [1976] and Angelier et al [1985].

Predictably, the shallow-rake faults which strike about N20°–45°E compose the largest subset of data incompatible with the solution because they strike within 10° to 15° of the computed maximum horizontal stress direction and the preferred orientation of primarily dip-slip faults. Slip on these shallow rake faults is not only incompatible with the normal faulting stress regime having an S_3 of N60°W but also incompatible with simple permutations of the maximum horizontal and the vertical stress because the strike of these strike-slip faults is so close to the maximum horizontal stress direction.

An inconsistent sense of displacement of the shallow-rake faults striking N20°–45°E further hampers the understanding of their significance: both right- and left-lateral offsets are observed. These apparently contradictory offsets may be attributable to (1) rotation of the regional principal stress field, (2) tectonic rotation about a vertical axis of blocks containing the faults, or (3) second-order local stress reorientations.

As discussed in the introduction, several workers have suggested a late Cenozoic rotation or change in orientation of the regional stress field in the southern Nevada area (Anderson and Ekren [1977]; Ander [1984]; see also Zoback et al. [1981]). However, all these authors have indicated only a clockwise change in rotation. The observation of both right-lateral and left-lateral offset on the N30°–45° strike-slip faults appears to rule out a simple clockwise change in stress orientation.

Paleomagnetic studies in southern Nevada have revealed several examples of the second explanation, block rotation about a vertical axis. At Yucca Mountain 35 km NW of Hampel Wash, Scott and Rosenbaum [1986] report a 13 m.y. old tuff unit displaying progressive clockwise rotation from north to south with the southern end rotated 30° relative to the northern end. Within the Lake Mead shear zone near Hoover Dam, Ron et al., [1986] reported 27 degrees of counterclockwise rotation in 11–12 Ma volcanic rocks. Ron et al. [1984] have proposed a model for local block rotation resulting from strike-slip faulting; their model predicts that internal rotation (accommodated on a conjugate set of strike-slip faults) occurs within regions bounded by major strike-slip faults. Applying this model to the Hampel Wash area which is bounded on the north and south by left-lateral oblique faults, one would expect an internal counterclockwise rotation. This counterclockwise rotation would be accommodated on smaller right-lateral faults which would rotate, along with the blocks they bound, from the orientation in which they developed.

As shown on Figure 4, most of the right-lateral faults of the data set strike approximately N-S (as expected in the modern stress regime) or are rotated clockwise from this position (to the NE); furthermore, the left-lateral faults appear to have rotated counterclockwise from their expected ENE direction. Thus, in a field example very similar to the conceptual model of Ron et al. [1984], the results appear incompatible with the model. A detailed paleomagnetic study has not been undertaken in this area and would be of considerable interest.

The final explanation of the inconsistent right-lateral and left-lateral offsets on NE striking faults, as being due to local stress reorientations, is always a potential source of noise in fault slip studies [e.g., Angelier, 1979, p. T20]. However, one would expect such noise to produce random rotations of the faults rather than the observed clockwise rotation of right-lateral faults and counterclockwise rotation of left-lateral faults.

SUMMARY

Fault slip data collected in a seismically active part of southern Nevada in an area bounded by relatively young left-lateral faults exhibit a bimodal distribution of rakes that indicates nearly pure strike-slip or pure normal dip-slip faulting. Normal dip-slip faults cluster about a N30°–35°E strike; whereas shallow-rake faults strike about a dominant node of N30°–45°E (which includes both right-lateral and left-lateral offset) and subordinate quasi-conjugate nodes of N66°–80°E (left-lateral offset) and N-to-NNE (right-lateral faults). An iterative inversion of the data indicates a best fitting deviatoric stress tensor characterized by a normal faulting stress regime (S_1 vertical) having principal stress axes in approximately horizontal and vertical planes and a least horizontal principal stress (S_3) orientation of N60°W. An intermediate value for $\phi \approx = 0.5$ indicates that the magnitude of the maximum horizontal stress lies approximately halfway between the magnitude of S_1 and S_3. The S_3 orientation is consistent with the inferred modern least horizontal principal stress orientation in the vicinity of the Nevada Test Site of N50°–70°W previously obtained from earthquake focal mechanisms, well bore breakouts, and hydraulic fracturing measurements. The intermediate value of ϕ indicates that both the quasi-conjugate strike slip and normal faulting may be compatible with deformation in a normal faulting stress regime. The maximum horizontal and vertical stress need not exchange magnitudes as suggested by Wright [1976] and Angelier et al. [1985].

The solution fits all the data well except for strike-slip faults that strike N30°–45°E, subparallel to the normal faults of the data set. The strike-slip offsets observed on these NE striking faults, as well as superposed sets of striae observed on some faults, suggest either rotations of the regional stress field or local block rotations within fault zones.

Aknowledgments. Jim Yount shared his understanding of the Rock Valley fault and Mark Gorden helped in data collection. This article benefited from helpful and sometimes

challenging comments by Ernie Anderson, Doc Bonilla, Ben Page, Ze'ev Reches, Hagai Ron, Joanne Stock, and George Thompson.

REFERENCES

Ander, H. D., Rotation of late Cenozoic extensional stresses, Yucca Flat region, Nevada Test Site, Nevada, Ph.D. thesis, 77 pp., Rice Univ., Houston, Tex., 1984.

Ander, H. D., F. M. Byers, Jr., and P. P. Orkild, Geology of the Nevada Test Site (Field Trip 10), in *Western Geological Excursions*, vol. 2, edited by Joseph Lintz, Jr., pp. 1–35, Department of Geological Sciences, Mackay School of Mines, Reno, Nev., 1984.

Anderson, R. E., and E. B. Ekren, Late Cenozoic fault patterns and stress fields in the Great Basin and westward displacement of the Sierra Nevada block: Comment, *Geology, 5*, 388–389, 1977.

Angelier, J., Determination of the mean principal directions of stress for a given population, *Tectonophysics*, 56, T17–T26, 1979.

Angelier, J., Tectonic analysis of fault slip data sets, *J. Geophys. Res., 89*, 5835–5848, 1984.

Angelier, J., B. Colletta, and R. E. Anderson, Neogene paleostress changes in the Basin and Range: A case study at Hoover Dam, Nevada-Arizona, *Geol. Soc. Am. Bull, 96*, 347–361, 1985.

Barnes, H., E. B. Ekren, C. L. Rodgers, and D. C. Hedlund, Geologic and tectonic maps of the Mercury quadrangle, Nye and Clark Counties, Nevada, scale 1:24,000, *U.S. Geol. Surv. Misc. Invest. Map Ser., Map I–1197*, 1982.

Burchfiel, B. C., Precambrian and Paleozoic stratigraphy of Spector Range quadrangle, Nye County, Nevada, *Am. Assoc. Pet. Geol. Bull., 48*, 40–56, 1964.

Byers, F. M., Jr., W. J. Carr, P. P. Orkild, W. D., Quinlivan, and K. A. Sargent, Volcanic suites and related cauldrons of Timber Mountain-Oasis Valley Caldera complex, southern Nevada: *U.S. Geol. Surv. Prof. Pap. 919*, 1–70, 1976.

Carr, W. J., Summary of tectonic and structural evidence for stress orientation at the Nevada Test Site: *U.S. Geol. Surv. Open-File Rep. 74–176*, 1–53, 1974.

Carr, W. J., Regional structural setting of Yucca Mountain, southwestern Nevada, and late Cenozoic rates of tectonic activity in part of the southwestern Great Basin, Nevada and California: *U.S. Geol. Surv. Open-File Rep., 84–854*, 1–109, 1984.

Frizzell, V. A., and M. L. Zoback, Striae on faults in Hampel Wash, southern Nevada, indicate least horizontal principal stress direction of N60°W: Eos *Trans. AGU, 66*, 1056, 1985.

Hinrichs, E. N., Geologic map of the Camp Desert Rock quadrangle, Nye County, Nevada, 1:24,000 scale, *U.S. Geol. Surv. Geol. Quadrangle Map, GQ–726*, 1968.

Kistler, R. W., Potassium-argon ages of volcanic rocks in Nye and Esmeralda Counties, Nevada, *Mem. Geol. Soc. Am. 10*, 251–262, 1968.

Rogers, A. M., S. C. Harmsen, W. J. Carr, and W. Spence, Southern Great Basin seismological data report for 1981 and preliminary data analysis, *U.S. Geol. Surv. Open-File Rep. 83–669*, 1–240, 1983.

Ron, H., R. Freund, Z. Garfunkel, and A. Nur, Block rotation by strike-slip faulting: Structural and paleomagnetic evidence: *J. Geophys. Res., 89*, 6256–6270, 1984.

Ron, H., A. Aydin, and A. Nur, Strike-slip faulting and block rotation in the Lake Mead fault system, *Geology, 4*, 1020–1023, 1986.

Scott, R. B. and J. G. Rosenbaum, Evidence of rotation about a vertical axis during extension at Yucca Mountain, Southern Nevada, *Eos, Trans. AGU, 67*, 358, 1986.

Springer, J. E., R. K. Thorpe, and H. L. McKague, Borehole elongation and its relation to tectonic stress at the Nevada Test Site, *Lawrence Livermore Lab. Rep., UCRL–53528*, 43 pp., 1984.

Stewart, J. H., and J. E. Carlson, Geologic map of Nevada, scale 1:500,000, *U.S. Geol. Surv.*, Reston, Va., 1978.

Stock, J. M., J. H. Healy, S. H. Hickman, and M. D. Zoback, Hydraulic fracturing stress measurements at Yucca Mountain, Nevada, and relationship to the regional stress field: *J. Geophys. Res., 90*, 8691–8706, 1985.

Vetter, U. R., and A. S. Ryall, Systematic change of focal mechanism with depth in the western Great Basin, *J. Geophys. Res., 88*, 8237–8250, 1983.

Wright, L., Late Cenozoic fault patterns and stress fields in the Great Basin and westward displacement of the Sierra Nevada block, *Geology, 4*, 489–494, 1976.

Yount, J. C., R. R. Shroba, C. R. McMasters, H. E. Huckins, and E. A. Rodriguez, Trench logs from a strand of the Rock Valley fault, Nevada Test Site, Nye County, Nevada, scale 1:10, *U.S. Geol. Surv. Misc. Field Studies Map MF–1824*, 1987.

Zoback, M. L., and M. D. Zoback, State of stress in the conterminous United States: *J. Geophys. Res., 85*, 6113–6156, 1980.

Zoback, M. L., R. E. Anderson, and G. A. Thompson, Cainozoic evolution of the state of stress and style of tectonism of the Basin and Range province of the western United States: *Philos. Trans. R. Soc. London, Ser. A, 300*, 407–434, 1981.

V. A. Frizzell, Jr., Western Regional Geology, U.S. Geological Survey, 2255 North Gemini Drive, Flagstaff, AZ 86001.

M. L. Zoback, Seismology, U.S. Geological Survey, Menlo Park, 94025.

(Received May 22, 1986;
revised December 8, 1986;
accepted December 12, 1986)